

---

---

NUCLEAR EXPERIMENTAL  
TECHNIQUE

---

---

# A Method for High-Resolution and High-Efficiency Spectroscopy of Ultracold Neutrons at a Small Energy Transfer and Low Scattering Probabilities

Yu. N. Pokotilovskii and G. F. Gareeva

*Joint Institute for Nuclear Research, ul. Joliot Curie 6, Dubna, Moscow oblast, 141980 Russia*

Received February 4, 2002

**Abstract**—Geometry and a method are proposed for spectral measurements of quasi-elastically reflected ultracold neutrons with an energy transfer of up to  $\sim 200$  neV and low scattering probabilities. This method is based on the use of a threshold detector moving in the gravitational field. The attainable energy resolution is 3–5 neV. A Monte Carlo simulation of the spectrometer was performed.

Ultracold (with energy up to  $\sim 250$  neV) neutrons (UCN) have the property to be reflected at any angle of incidence from the surface of a substance with a positive scattering length and, thereby, be stored in a closed space for a long period of time (hundreds of seconds). This property was shown theoretically [1] and demonstrated by the experiment [2]. The experimental and theoretical findings in this field and the use of UCN in basic research of neutron physics have been described in reviews and monographs [3].

The interactions of UCN in their reflection by the substance surface are conventionally analyzed on the assumption that the reflection proceeds elastically, with the exception of rare events (probability  $10^{-3}$ – $10^{-5}$ ) when neutrons disappear from the storage volume as a result of their capture by nuclei of the medium or the acquisition, while scattering, of the energy  $E \sim kT \gg E_0$  ( $T$  is the temperature of the surface, and  $E_0$  is the initial neutron energy) through thermal vibrations of atoms in the medium. Note that there is a significant discrepancy (by a factor of  $10^2$ – $10^3$ ) between the loss factors observed in the UCN reflection from cold (10–80 K) solid surfaces and those computed according to the present-day theory of UCN reflection by a surface. This is currently the essence of the UCN-storing problem [4].

Interest has arisen lately in the effects of small changes in the UCN energy ( $\Delta E \leq E_0$ ) upon reflection by surfaces. These effects observed in experiments are described in [5–13]; possible physical mechanisms that might basically be responsible for them are considered in [14–18]. It has been ascertained that the probability of small changes in the energy of a neutron upon its reflection by a wall; i.e., more precisely, the probability that a neutron with an initial energy of 50 to 100 neV will change it by a value of 50–100 neV, lies between  $10^{-5}$  and  $10^{-8}$  (the data vary from paper to paper). For better insight into the mechanism of such effects, one

needs reliable high-resolution (a few nanoelectronvolts) spectroscopy of these energy variations; i.e., it is necessary to measure the differential probability  $dw/d\varepsilon$  ( $\varepsilon$  is the energy of a neutron transferred upon its reflection). The smallness of the relative effect in comparison with the dominating capture processes, especially, inelastic scattering with a large energy transfer resulting in the loss of a neutron from the storage volume, dictates the requirement that the detection efficiency for a neutron that has changed its energy should be the highest possible. In the references in which these effects were observed, the detection efficiency of scattered neutrons was only a few percent because of the geometric features of the setup; moreover, spectroscopy of small changes in the energy of scattered UCN was not involved. That is why it is impossible to estimate the behavior of  $dw/d\varepsilon$  in the imparted-energy range of interest  $\varepsilon = 0$ –200 neV.

We describe the geometry of the setup and the method of high-transmission UCN spectroscopy permitting the detection of scattered neutrons with up to 100% efficiency over a 0 to 200-neV range of imparted energies. This method is based on the simultaneous use of a threshold detector and gravitational acceleration to vary the energy of the detected neutrons. In this respect, it is similar to the method we used to measure the energy dependence of the efficiency of various UCN detectors [19] and analyze the energy dependence of the probability of UCN losses in closed traps coated with hydrogen-free oil—a Fomblin-type fluorocarbon polymer [20]. The energy resolution of the method is 3–5 neV. The spectrometer operation was simulated by the Monte Carlo method.

A diagram of the setup is shown in Fig. 1. Ultracold neutrons travel over a neutron guide  $1$  through the membrane 2, shutting it off, and reach the scattering chamber 3. The membrane 2 with a boundary energy

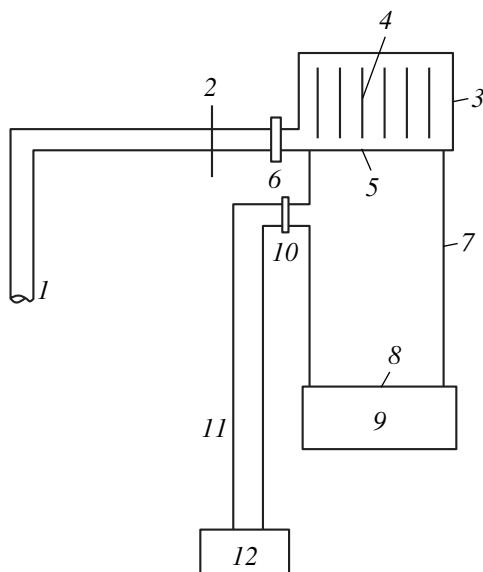


**Fig. 1.** Diagram of the spectrometer: (1) feeding neutron guide; (2) membrane putting a lower bound on the original neutron spectrum; (3) scattering chamber; (4) sample; (5) membrane putting an upper bound on the original neutron spectrum and a lower bound on the spectrum of scattered neutrons; (6) valve; (7) vertical (accelerating) neutron guide; (8) membrane putting a lower bound on the spectrum of scattered and accelerated neutrons; (9) neutron detector; (10) valve; (11) vertical (accelerating) neutron guide; and (12) neutron detector.

for UCN  $E_n$  sets a lower limit on the spectrum of neutrons entering the chamber. A sample under investigation 4 is located inside the chamber. The sample has an extended surface (in order to increase the effect) in the form of, e.g., a roll or a stack of foils made of material under investigation or coated with it. The bottom of the scattering chamber is covered with a thin ( $<100 \mu\text{m}$ ) membrane 5 with the boundary energy for UCN  $E_1$ . In the case where the auxiliary devices located in front of the entrance to the chamber form the UCN spectrum so that the UCN energy in the chamber on the level of membrane 5 is  $E_1$  or less, the measurements can be carried out in a stationary neutron flux. Otherwise, the experiment should be conducted in a cyclic regime (as was done in [5–12]) using the valve 6 at the entrance in the chamber 3. In this case, within the time determined experimentally, neutrons with an energy  $>E_1$ , locked with the valve 6 in the chamber 3, disappear from this chamber through the membrane 5, are accelerated by the gravitational field in the vertical neutron guides 7 and 11 (while the valve 10 is open), and are then detected by the detectors 9 and 12 (the need for the two neutron guides 7 and 11, as well as for the valve 10 is explained below).

The background neutrons (with energies above the barrier) with an initial energy in the chamber of  $>E_1$  are separated from the major portion of the neutron spectrum with an energy of  $<E_1$ , whose scattering is inves-

tigated, by analyzing, similarly to [5–12], the time dependence of the responses of the neutron detectors 9 and 12. This dependence represents the characteristic time of a neutron's escape from the chamber 3. The characteristic time is defined by the sum of the probabilities that the neutron with an energy  $>E_1$  traverses the membrane 5 and that the neutrons disappear from the chamber due to inelastic processes. Since the first probability exceeds the second probability significantly (this is the principal requirement for experiments which are carried out in nonstationary regime), this allows the process of transferring small energy portion to be detected after all the primary neutrons with an energy  $>E_1$  have left the chamber 3 through the membrane 5 within a relatively short characteristic time (at that time, the valve 10 is closed).

These setup components, as well as the method for detecting neutron scattering, are similar in many respects to the experimental setup [6, 8]; however, they have a number of essential differences. For example, the element forming the primary-neutron spectrum in the setup [6, 8] is a polyethylene absorber located at the top of the scattering chamber. The degree to which the neutron-absorption coefficient of polyethylene differs from unity displays the quality of clearing of the initial spectrum from foreign neutrons capable of imitating a small change in the neutron energy upon reflection from the sample under study. The dependence of this coefficient on the neutron energy is difficult to measure, and it has never been determined. It is quite possible that the surface of polyethylene is coated with a thin film of impurities, e.g., oil, which may significantly impair the absorbing properties of polyethylene. Cleaning it from impurities by heating in vacuum is impossible. Figure 2 presents the calculated factor of neutron reflection from polyethylene as a function of the normal component of the neutron velocity for varying thicknesses of the Fomblin film (fluorocarbon polymer oil, boundary energy 106 neV) on the surface. We see that the presence of the film results in noticeable neutron reflection and, hence, in the degradation of the degree of the spectrum clearing from foreign above-boundary neutrons (with energies above the boundary). Figure 3 presents the lifetimes of these neutrons simulated by the Monte Carlo method (the simulation conditions are described below) in the geometry similar to the geometry of the experiments [6, 8]: the chamber for the spectrum formation and subsequent storage of UCN and heated neutrons measures  $20 \times 20$  cm, and the polyethylene absorber is located at a height of 52 cm. The data obtained from these lifetimes (Fig. 4) characterize the degree of survival of above-boundary neutrons within a time interval of 55 s, which is the standard time of the formation of the initial neutron spectrum in the experiments [6, 8]. The simulation results (Figs. 2–4) demonstrate that the noticeable impurity of above-boundary neutrons remains in the spectrum after its clearing from

them, which may imitate the effect in question or affect the probability of quasi-elastic UCN heating.

In the proposed technique, the passage of neutrons through the membrane 5—the key element of the setup and the spectrum former which puts the upper boundary on the spectrum of primary neutrons and the lower boundary on the spectrum of detected scattered neutrons—is easily determined by experiment. When this filter is located on the floor of the chamber, the spectrum is cleared with a no lesser efficiency as it is in the case when an unpolluted polyethylene absorber is placed at the chamber’s ceiling. This fact is illustrated by the simulation results for the chamber 3 with dimensions of  $14 \times 14 \times 20$  cm presented in Fig. 5. We see that the average lifetimes of above-boundary neutrons do not exceed the lifetimes for the spectrum cleared with polyethylene (Fig. 3); however, in this case, the effect of pollutant films at the membrane surface is insignificant. This is due to the higher energy of neutrons colliding with the filter and the higher collision frequency.

The effective surface of the membrane in front of the detector in [6, 8] is a fraction of a percent of the scattering-chamber surface; hence, the probability of detecting a neutron scattered with a change in the energy is small. In the proposed version, the area of the membrane 5 used for the initial energy discrimination of scattered neutrons is tens of percent of the chamber surface 3 and, as the Monte Carlo simulation shows, the probability of detecting a neutron scattered with a small increase in its energy ( $\Delta E \leq E_0$ ) approaches 100%.

The important elements of the proposed system for measuring the differential probability of UCN scattering with a small energy transfer are the vertical neutron guide 7 of height  $h$  and the second membrane 8 located immediately in front of the sensitive volume of the neutron detector 9. If the boundary energy of the second membrane 8 is  $E_2$ , the detector can detect neutrons whose energy at the level of membrane 5 is

$$E = E_0 + \varepsilon > E_2 - mgh \quad (1)$$

(besides the obvious condition  $E > E_1$ ), where  $E_0$  is the original neutron energy (before the quasi-elastic collision) and  $\varepsilon$  is the energy imparted in scattering.

The operating range of imparted energies  $\varepsilon$  is bounded from above by the condition of zero neutron loss in the neutron guide 7 due to the excess of its boundary energy  $E_b$ ,

$$E = E_0 + \varepsilon < E_b - mgh. \quad (2)$$

As the detailed simulation shows, this second condition is not stringent. Hence, varying  $E_2$  and (or)  $h$  (the latter can be done without spectrometer decompression), it is possible to span a wide range of imparted energies while measuring the integral energy spectrum of neutrons scattered in the chamber 3 with a small energy transfer.

Consider practical examples. It is convenient to select (from practical considerations) the following

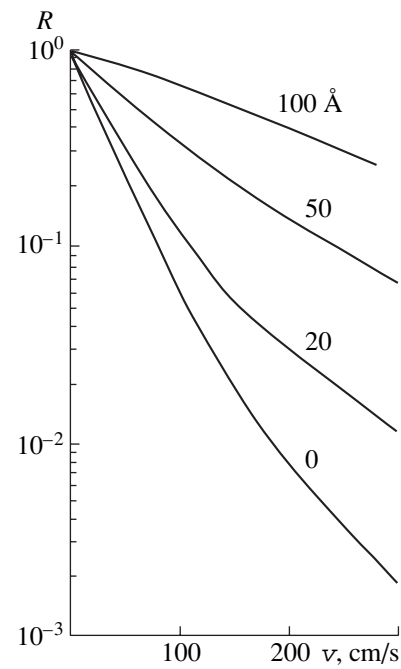


Fig. 2. Neutron-reflection coefficient  $R$  of polyethylene, obtained from the quantum-mechanical calculation, versus the normal component of neutron velocity  $v$  under different assumptions on the film thickness (figures near the curves) of Fomblin (fluorocarbon polymer oil, boundary energy 106 neV) on the polyethylene surface.

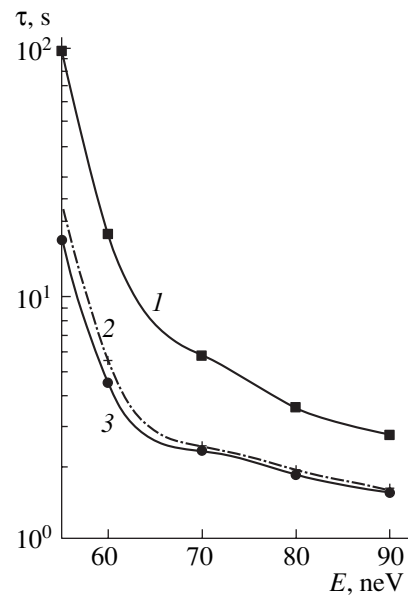
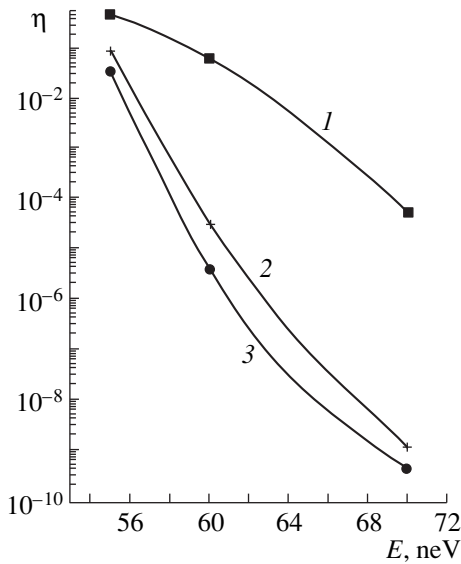
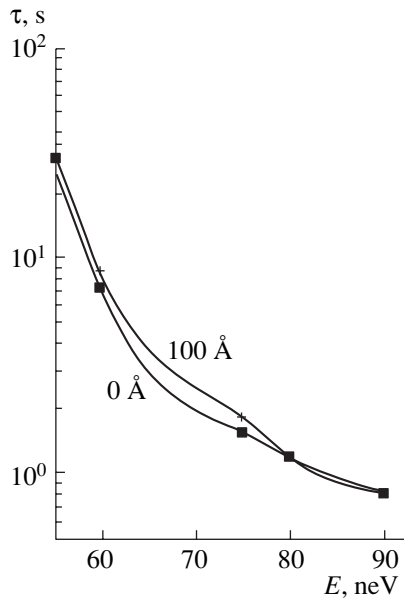


Fig. 3. Lifetimes of neutrons with energies above the boundary value, computed by the Monte Carlo method, as a function of their energy in the geometry similar to the experiments [6, 8], for (1) polyethylene with a 100-Å oil film on the surface, (2) unpolluted polyethylene, and (3) ideal absorber. The chamber measures  $20 \times 20$  cm; the polyethylene absorber is located at a height of 52 cm; the UCN-loss factor in collisions with the walls is  $\eta = 2 \times 10^{-4}$ ; and the boundary energy is 200 neV.



**Fig. 4.** The degree of “survival” of neutrons with energies above the boundary value within a time of 55 s with (1) polyethylene with a 100-Å oil film on the surface, (2) unpolluted polyethylene, and (3) ideal absorber used as spectrum formers.



**Fig. 5.** Lifetimes of neutrons with energies above the boundary value, computed by the Monte Carlo method, as a function of their energy in the proposed geometry of the spectrometer for different values of oil-film thickness (figures near the curves) at the surface of Al membrane. The chamber dimensions are  $14 \times 14 \times 20$  cm. The UCN loss factor in collisions with the walls is  $\eta = 2 \times 10^{-4}$ ; the boundary energy is 200 neV.

boundary energies:  $E_1 = 54$  neV (a thin aluminum membrane), as it was done in the experiments [6, 8], or  $E_1 = 79$  neV (zirconium membrane);  $E_b = 250$  neV (beryllium coating). The following values of the bound-

ary energies may be selected for the membrane 8:  $E_2 = 167$  neV (copper, zirconium) or  $E_2 = 94$  neV (germanium coating of an aluminum or zirconium membrane). Other variants may also be used. For  $E_2 = 167$  neV, by varying  $h$  from 0 to 81 cm, it is possible to accomplish the integral spectroscopy of neutrons scattered in the chamber 3 and passed through the membrane 5 over an energy range  $83 < E < 167$  neV (the neutron energy changes by 1.0255 neV in the gravitational field at a height of 1 cm). For  $E_2 = 94$  neV ( $h = 0$ –38 cm), this range is  $55 < E < 94$  neV. Hence, using a set of two membranes, it is possible to span a 55- to 167-neV energy range of stray neutrons. However, according to the simulation results (Fig. 6), it appears to be much wider.

The spectrometer was simulated by the Monte Carlo method. Neutrons were taken to be randomly incident on the surface of the membrane 5 and directed downwards with an isotropic angular distribution. The neutron path in the neutron guide 7 was simulated strictly with allowance for the gravity force; incidentally, the character of angular distribution of neutrons reflected from the walls of the neutron guide was assumed to be specular, diffuse, or combined. The quantitative results showed a weak dependence on this selection. The absorption of neutrons upon their collisions with the neutron-guide wall was taken into account. The probability that neutrons with energies below the barrier were absorbed was described by the known dependence [3]

$$\mu = \frac{2\eta x}{\sqrt{1-x^2}}, \quad (3)$$

where  $\eta$  is the loss factor  $x = v_{\perp}/v_b$ ,  $v_{\perp}$  is the neutron-velocity component perpendicular to the wall, and  $v_b$  is the boundary velocity in the neutron guide ( $x < 1$ ).

The probability that a neutron with an energy above the barrier ( $v_{\perp} > v_b$ ) penetrated into the wall was calculated according to the expression from quantum mechanics

$$w = \frac{4x\sqrt{x^2-1}}{2x^2-1+2x\sqrt{x^2-1}}. \quad (4)$$

The absorption of neutrons in the membrane 8 and their repeated reflection by its boundaries were taken into account. The efficiency of detecting a neutron that went through the membrane 8 was taken to be 100%.

Figure 6a presents the neutron-detection efficiency of the detector with the copper membrane 8 for different height  $h$  of the neutron guide 7 as a function of neutron energy on the level of membrane 5. The following values of parameters were used in the calculation: the neutron guide was  $14 \times 14$  cm;  $\eta = 2 \times 10^{-4}$ ; the probability of diffuse reflection by the neutron-guide surface was defined by the expression

$$w = \cos\theta, \quad (5)$$

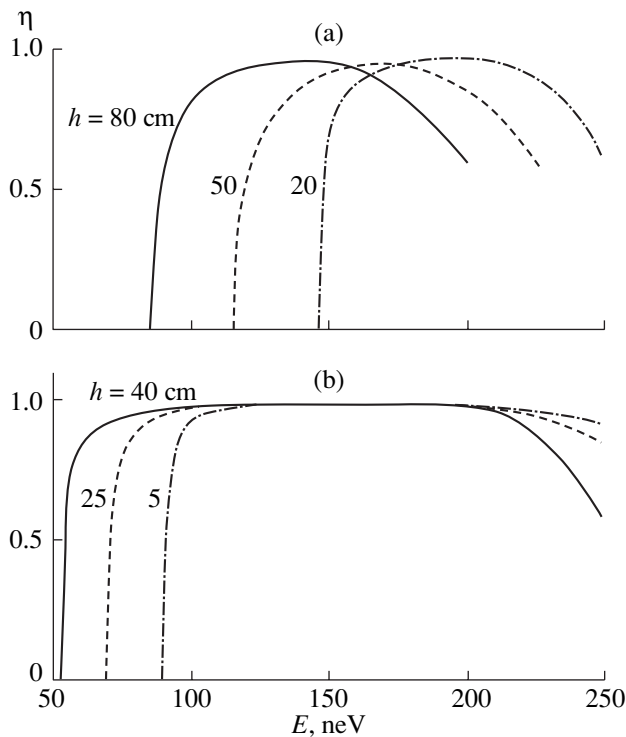


**Fig. 6.** Detection efficiency, simulated by the Monte Carlo method, for UCN scattered in the chamber as a function of their energy for different positions of the analyzing membrane (figures near the curves) (a) made of copper and (b) with Ge coating.

where  $\theta$  is the angle of the vector of incident-neutron velocity with the normal to the surface. The membrane 8 was assumed to be 50  $\mu\text{m}$  thick (aluminum) with a thin surface layer of copper (or germanium).

The simulation results show a high resolution of this spectrometer (the FWHM of the threshold curves is 3–5 neV) and a high detection efficiency for a neutron travelling in the neutron guide 7. In this case, as the plots show, the detection efficiency decreases rather smoothly with the energy of neutrons, whose acceleration in the neutron guide 7 should result in an excess of the neutron-guide boundary energy  $E_b$  and their loss through the penetration into the guide's walls. The simulation also demonstrates that, for a certain (dozens of nanoelectronvolts) energy range of scattered neutrons, when the neutron energy at the bottom of the neutron guide 7 exceeds its boundary energy  $E > E_b$ , passing of neutrons through the detector membrane dominates over the loss in the neutron guide.

The results of similar calculations for the membrane 8 coated with a thin germanium layer are given in Fig. 6b.

The theoretical lifetimes of neutrons in the neutron guide 7 are presented in Fig. 7 as a function of their energy on the level of membrane 5. The simulation shows a sharp decrease in the lifetime as soon as the neutron energy starts exceeding  $E_2$  (the boundary energy for the membrane 8) through the acceleration in

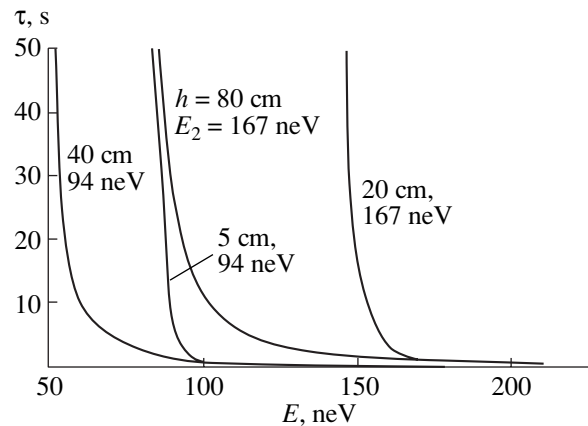


**Fig. 7.** UCN lifetimes in the neutron guide, simulated by the Monte Carlo method, versus their energy for different positions of the analyzing membrane.  $E_2$  is the boundary energy for membrane 8.

the gravitational field. Neutrons, whose energy is insufficient to pass through the membrane 8, but whose lifetime in the neutron guide is long (Fig. 7), are then removed by opening the valve 10 and detected by the detector 12.

## REFERENCES

1. Zel'dovich, Ya.B., *Zh. Eksp. Teor. Fiz.*, 1959, vol. 36, no. 6, p. 1952.
2. Lushchikov, V.I., Pokotilovskii, Yu.N., Strelkov, A.V., and Shapiro, F.L., *Pis'ma Zh. Eksp. Teor. Fiz.*, 1969, vol. 9, no. 1, p. 40.
3. Steyerl, A., in *Springer Tracts in Modern Physics*, Berlin: Springer, 1977, vol. 80, p. 57; Golub, R. and Pendlebury, J.M., *Rep. Prog. Phys.*, 1979, vol. 42, p. 439; Ignatovich, V.K., *Fizika ul'trakhodnykh neutronov*, Moscow: Nauka, 1986. Translated under the title *The Physics of Ultracold Neutrons*, Oxford: Clarendon, 1990; Golub, R., Richardson, D.J., and Lamoreaux, S., *Ultracold Neutrons*, Bristol: Adam Hilger, 1991.
4. Alfimenkov, V.P., Nesvizhevski, V.V., Serebrov, A.P., et al., *Preprint of Inst. of Nuclear Physics, USSR Acad. Sci.*, Gatchina, 1991, no. 1729; *Pis'ma Zh. Eksp. Teor. Fiz.*, 1992, vol. 55, p. 92 [*JETP Lett.* (Engl. transl.), 1992, vol. 55, p. 84]; *Preprint of Inst. of Nuclear Physics, Russ. Acad. Sci.*, Gatchina, 1992, no. 1756.
5. Bondarenko, L., Geltenbort, P., Korobkina, E., et al., *ILL Experimental Report*, 1997, no. 3-14-44; *Pis'ma Zh. Eksp. Teor. Fiz.*, 1998, vol. 68, no. 9, p. 663.
6. Nesvizhevsky, V.V., Geltenbort, P., Strelkov, A.V., and Iaydjiev, P., *ILL Annual Report*, 1997, p. 62; *JINR Commun.* (Dubna), 1998, no. P3-98-79.
7. Arzumanov, S., Bondarenko, L., Chernyavsky, S., et al., Abstracts of Papers, *Proc. Int. Seminar on Interaction of Neutrons with Nuclei, ISINN-6*, Dubna, 1998, p. 108; Bondarenko, L., Korobkina, E., Morozov, V., et al., *ILL Experimental Report*, Grenoble, France, 1997, no. 3-14-44.
8. Nesvizhevskii, V.V., Strelkov, A.V., Gel'tenbort, P., and Yaidzhiev, P., *Yad. Fiz.*, 1999, vol. 62, no. 5, p. 832.

9. Lychagin, E.V., Muzychka, A.Yu., Nesvizhevskii, V.V., *et al.*, *Yad. Fiz.*, 2000, vol. 63, no. 4, p. 609.
10. Geltenbort, P., Nesvizhevsky, V.V., Kartashov, D.G., *et al.*, *Pis'ma Zh. Eksp. Teor. Fiz.*, 1999, vol. 70, p. 175.
11. Nesvizhevsky, V.V., Lychagin, E.V., Muzychka, A.Y., *et al.*, *Phys. Lett. B*, 2000, vol. 479, p. 353.
12. Nesvizhevsky, V.V., Strelkov, A.V., Geltenbort, P., and Iaydjiev, P., *Eur. Phys. J.: Appl. Phys.*, 1999, vol. 6, p. 151.
13. Serebrov, A.P., Butervorf, D., Varlamov, V.E., *et al.*, *Preprint of Inst. of Nuclear Physics, Russ. Acad. Sci., Gatchina*, 2001, no. 2438.
14. Pokotilovski, Yu.N., *Eur. Phys. J. B*, 1999, vol. 8, p. 1.
15. Pokotilovski, Yu.N., *Phys. Lett. A*, 1999, vol. 255, p. 173.
16. Pokotilovskii, Yu.N., *Pis'ma Zh. Eksp. Teor. Fiz.*, 1999, vol. 69, no. 2, p. 81 [*JETP Lett.* (Engl. transl.), 1999, vol. 69, p. 91].
17. Barabanov, A.L. and Belyaev, S.T., *Yad. Fiz.*, 1999, vol. 62, no. 1, p. 824; *Nucl. Instrum. Methods Phys. Res. A*, 2000, vol. 440, p. 704.
18. Ignatovich, V.K. and Utsuro, M., *Nucl. Instrum. Methods Phys. Res. A*, 2000, vol. 440, p. 709.
19. Novopoltsev, M.I. and Pokotilovski, Yu.N., *Nucl. Instrum. Methods*, 1980, vol. 171, p. 497.
20. Richardson, D.J., Pendlebury, J.M., and Iaydjiev, P., *Nucl. Instrum. Methods Phys. Res. A*, 1991, vol. 308, p. 568.